NUMERECAL MODELING OF THE PROGRESSIVE COLLAPSE OF FRAMED STRUCTURE BY USING IMPROVED APPLIED ELEMENT METHOD

Said ELKHOLY[1] and Kimiro MEGURO[2]

ABSTRACT: Applied Element Method (AEM) is recognized as a powerful tool for analyzing the structural behavior from early stage of loading up to the total collapse occurs. At first a brief overview of Applied Element Method's formulation is presented. Subsequently, a new improvement for Applied-Element Method has been introduced and employed in the development of novel numerical solutions for analysis of failure and collapse of high-rise-steel structures under hazardous loads such as arising from blast loading. In the improved method, new element type has been presented and employed. The verification examples indicate that improved AEM has better accuracy, needs less computational effort, and has a wider applicability for structural analysis, especially for studying high rise steel buildings than conventional methods. The proposed numerical method also takes into account contact-impact, recontact and inertia effects. Collapse analysis for a high-rise steel structure has been presented as an example.

Key Words: Numerical simulation, Progressive Failure, Applied Element Method, Improved AEM

INTRODUCTION

The collapse of the World Trade Centre, on September, 2001 was caused by a series of very complex events, involving tremendous impact to the structure, fire explosion and resulting heat. Responding like this terrorist attacks around the world, numerous researchers[1)-4)] are seeking new methods for simulating the collapse of those towers to understand and prevent progressive collapse of such high-rise buildings. It is very difficult or impossible to follow the complete collapse behaviors using numerical methods based on continuum material like **FEM** and **BEM**. Few numerical methods can deal with collapse analysis, like **EDEM**[5)] and AEM[6)-14)], which can simulate collapse behavior of reinforced concrete structures. However none of them had been used for steel structures case.

The application of the Applied Element Method (**AEM**) to structural Analysis is recognized as a powerful tool for analyzing the structural behavior from early stage of loading up to the total collapse occurs. It has been used successfully with different type of material like reinforced concrete, soil1[4)] and masonry. However, in order to guarantee good accuracy of the solution in case of steel structure, the number of elements used to model a structure may be very large indeed. So, it is necessary to search for a new technique requiring less computer time and effort to model a structure.

For that reason, the authors attempted to improve the existing code of **AEM** to be able to follow the behavior of steel structure up to the complete collapse by modifying element type. The new element reduces the size of problem, thus further reducing the CPU time required. The accuracy of the new element is tested and validated under both static and dynamic loading situations. The proposed numerical method also takes into account contact-impact, recontact and inertia effects. Collapse

[1] Doctoral Student, Institute of Industrial Science, The University of Tokyo

[2] Assoc. Professor, International Center for Urban Safety Engineering, Institute of Industrial Science, The University of Tokyo

analysis for a high-rise steel structure has been introduced in this paper. The numerical simulation explains to some extend the failure mechanism of the North Tower in World Trade Centre tower.

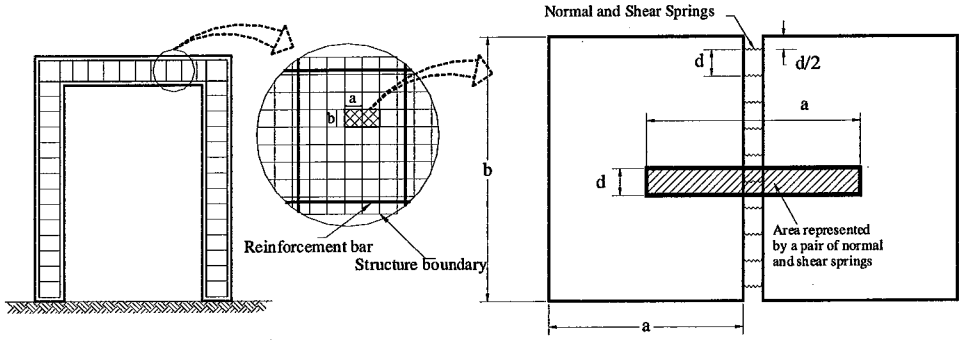

(a) Element generation for AEM (b) Spring distribution and area of influence of each pair of springs

Fig. 1 Modelling of structure to AEM[6)]

A BRIEF INTRODUCTION TO APPLIED ELEMENT METHOD

Applied Element Method (**AEM**)[6) ~ 10)], which was developed recently as a general method for structural analysis in both small and large displacement ranges has shown a good accuracy predicting the structural behavior from no loading stage till the complete collapse. In **AEM**, structure is modeled as an assembly of small square elements that are made by dividing of the structure virtually, as shown in **Fig. 1 (a)**. The elements are assumed to be infinitely rigid in order to reduce the computational cost. The two elements shown in **Fig. 1(b)** are assumed to be connected by pairs of normal and shear springs located at contact locations that are distributed around the element edges. Each pair of springs totally represents stresses and deformations of a certain area (hatched area in **Fig. 1 (b)**) of the studied elements. The springs carried out the microscopic material properties, such as stiffness and yield strength. The spring stiffness is determined as shown in **Eq. (1)**, assuming homogeneous thickness of element:

$$K_n = \frac{E \times d \times T}{a} \quad \text{and} \quad K_s = \frac{G \times d \times T}{a} \tag{1}$$

where, d is the distance between springs, T is the thickness of the element and "a" is the length of the representative area, E and G are the Young's and shear modulus of the material, respectively. The above equation indicates that each spring represents the stiffness of an area (d x T) with length "a" of the studied material. In case of reinforcement, this area is replaced by that of the reinforcement bar. The above equation indicates that the spring stiffness is calculated as if the spring connects the element centerlines.

Three degrees of freedom are assumed for each element. These degrees of freedom represent the rigid body motion of the element. Although the element motion is a rigid body

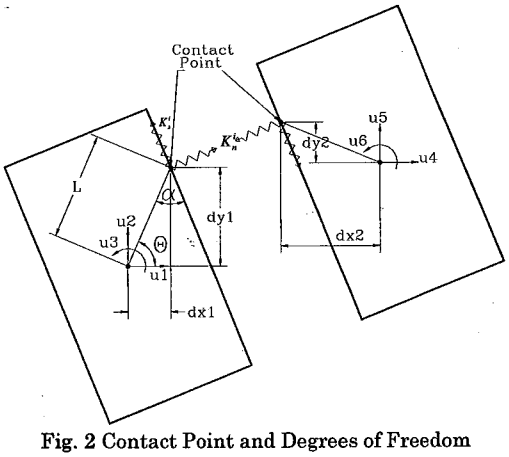

Fig. 2 Contact Point and Degrees of Freedom

motion, its internal stress and deformations can be calculated by the spring deformation around each element. This means that although the element shape doesn't change during analysis, the behavior of assembly of elements is deformable.

The two elements shown in **Fig. 2** are assumed to be connected by only one pair of normal (stiffness: K_n) and shear (stiffness: K_s) springs. The values of (dx and dy) correspond to the relative coordinate of the contact point with respect to the centroid. To have a general stiffness matrix, the location of elements and contact springs are assumed in a general position. The stiffness matrix components corresponding to each degree of freedom are determined by assuming a unit displacement in the studied direction and by determining forces at the centroid of each element. The element stiffness matrix size is only (6 x 6). **Eq. (2)** shows the components of the upper left quarter of the stiffness matrix. All used notations in this equation are shown in **Fig. 2**. It is clear that the stiffness matrix depends on the contact spring stiffness and the spring location.

$$\left[\begin{array}{c|c|c} \begin{array}{l}\mathrm{Sin}^2(\theta+\alpha)K_n\\ +\mathrm{Cos}^2(\theta+\alpha)K_s\end{array} & \begin{array}{l}-K_n\mathrm{Sin}(\theta+\alpha)\mathrm{Cos}(\theta+\alpha)\\ +K_s\mathrm{Sin}(\theta+\alpha)\mathrm{Cos}(\theta+\alpha)\end{array} & \begin{array}{l}\mathrm{Cos}(\theta+\alpha)K_sL\mathrm{Sin}(\alpha)\\ -\mathrm{Sin}(\theta+\alpha)K_nL\mathrm{Cos}(\alpha)\end{array} \\ \hline \begin{array}{l}-K_n\mathrm{Sin}(\theta+\alpha)\mathrm{Cos}(\theta+\alpha)\\ +K_s\mathrm{Sin}(\theta+\alpha)\mathrm{Cos}(\theta+\alpha)\end{array} & \begin{array}{l}\mathrm{Sin}^2(\theta+\alpha)K_s\\ +\mathrm{Cos}^2(\theta+\alpha)K_n\end{array} & \begin{array}{l}\mathrm{Cos}(\theta+\alpha)K_nL\mathrm{Cos}(\alpha)\\ +\mathrm{Sin}(\theta+\alpha)K_sL\mathrm{Sin}(\alpha)\end{array} \\ \hline \begin{array}{l}\mathrm{Cos}(\theta+\alpha)K_sL\mathrm{Sin}(\alpha)\\ -\mathrm{Sin}(\theta+\alpha)K_nL\mathrm{Cos}(\alpha)\end{array} & \begin{array}{l}\mathrm{Cos}(\theta+\alpha)K_nL\mathrm{Cos}(\alpha)\\ +\mathrm{Sin}(\theta+\alpha)K_sL\mathrm{Sin}(\alpha)\end{array} & \begin{array}{l}L^2\mathrm{Cos}^2(\alpha)K_n\\ +L^2\mathrm{Sin}^2(\alpha)K_s\end{array} \end{array}\right] \quad (2)$$

IMPROVED APPLIED ELEMENT METHOD

Although the conventional **AEM** used in different engineering field had shown highly accuracy and applicability like reinforced concrete[11)-12)], soil[13)]and masonry[14)] few applications are difficult to handle like huge steel structure case. Using the current version of **AEM**, elements with very small size should be used to follow the rapped change in the thickness especially with the flanged cross sections (like I Shape, Channel, and Boxed sections), since the element should be chosen to fit the flange thickness.

In improved method more flexibility was added to **AEM** to be able to use different characteristic for each spring to match any change in the thickness in any part of structure cross sections. That kind of modification allows using element with large size, having the same cross sectional parameter like normal, shear and bending stiffness. For that reason, the normal and shear stiffness for each spring can be determined by **Eq. (3)**, which is more generalized than **Eq. (1)**.

$$K_n^i = \frac{E \times d \times T_n^i}{a} \quad \text{and} \quad K_s^i = \frac{G \times d \times T_s^i}{a} \quad (3)$$

where: T_n^i and T_s^i are the thickness represented by the spring i for normal and shear cases, respectively. That difference in the value of T_n^i and T_s^i owes to the change in effective area for both of normal and shear directions. That change in stiffness values allow us to simulate different characteristics of the cross section (Axial area, Shear area, and Bending stiffness).

Although in this method we can change the characteristics of all springs surrounding any element, in practical use, the changing in the corner springs only can be done in case of steel flanged sections. Cross-sections can be simulated. From **Fig. 3**, we can see that changing in the ratios of (K1/K2) and (K3/K4) can control on the

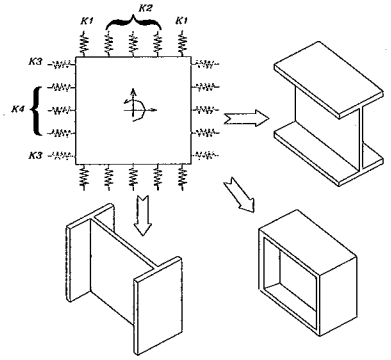

Fig. 3 Element shape for Improved AEM

stiffness of any element. That kind of improvement allows using many different flanged steel sections like I-beam, Box and Channel cross sections, as shown **Fig. 4**. Moreover, the element size may be chosen as the height of each cross section. That means elements with large size can be used which decrease the required number of elements and **CPU** time.

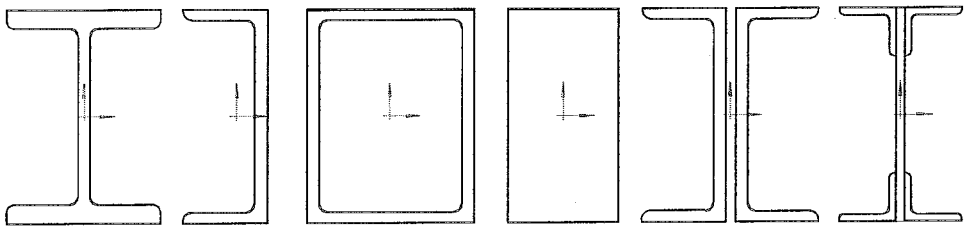

Fig. 4 Some Cross Sections can be directly used with Improved AEM

DYNAMIC ANALYSIS OF STRUCTURE BY USING IMPROVED AEM

The general differential equation of motion, governing the response of structure in small deformation range[15], can be shown to be:

$$[M]\{\Delta\ddot{U}\}+[C]\{\Delta\dot{U}\}+[K]\{\Delta U\}=\Delta f(t)-[M]\{\Delta\ddot{U}_G\} \tag{4}$$

where: [M] is mass matrix; [C] is the damping matrix; [K] is the nonlinear stiffness matrix; Δf(t) is the incremental applied load vector; $\{\Delta\ddot{U}\},\{\Delta\dot{U}\},\{\Delta U\}$, and $\{\Delta\ddot{U}_G\}$ are the incremental acceleration, velocity, acceleration, and gravity acceleration vectors, respectively.

In IAEM, the mass matrix and the polar moment of inertia of each element have been idealized as lumped at the element centroid. The corresponding lumped mass in each DOF direction can be calculated by summing the effect of small segmental mass represented by each spring considering the change of springs' thickness. **Eq. 5** represents the value of lumped mass in each degree of freedom direction.

$$\begin{bmatrix} M1 \\ M2 \\ M3 \end{bmatrix} = \begin{bmatrix} D^2 * t_{av} * \rho \\ D^2 * t_{av} * \rho \\ \dfrac{D^4 \cdot \rho}{nsp} \cdot \sum_{i=1}^{i=nsp} \left(\dfrac{t_i^x}{12} + \dfrac{t_i^y}{12}\right) \end{bmatrix} \tag{5}$$

where: D is the element size; t_{av} is the average thickness of the element; ρ the density of the material considered. It should be noticed that the [M1] and [M2] are corresponding to the element mass and [M3] is corresponding to the element polar moment of inertia about the centroid. Although the mass is lumped at the centroid of each element, its effect is very near to distributed mass systems if the element size is small.

LARGE DISPLACEMENT ANALYSIS WITH IMPROVED AEM

The concept of large displacement analysis has been introduced by Tagel-Din and Meguro (2002)[16].According to their concept, the **AEM** can follow the large deformation under both static and dynamic load by slight change in the equation of motion. The basic idea is to add two vectors R_m and R_G to the general equations of motion in both static and dynamic loading case. Where R_m represents the residual force vector due to cracking and incompatibility between strain and stress of each spring; and R_G the residual force vector due to geometrical changes in structure during loading. **Eq. 6** shows the new equation of motion in static load case.

$$[K]\{\Delta U\} = \Delta f + R_m + R_G \tag{6}$$

where Δf is the incremental load vector.

By assuming R_m and R_G equal to null and solve **Eq. 6** to get ΔU, the structural geometry can be modified according to the calculated incremental displacements. According to the modification of

geometry of structure and checking the occurrence of cracks new values for R_m and R_G can be calculated. Using those values for recalculate the incremental displacement ΔU considering the stiffness changes due to cracking and yielding. And repeat the entire process.
It should be emphasized that this technique can be used in case of large displacement behavior under dynamic loading condition. The general dynamic equation of motion in large displacement case is represented by **Eq. 7**.

$$[M]\{\Delta\ddot{U}\} + [C]\{\Delta\dot{U}\} + [K]\{\Delta U\} = \Delta f(t) + R_m + R_G \tag{7}$$

Analyzing the structure subjected to dynamic loading can allow us to follow both geometrical changes of the structure and rigid body motion during failure.

ILLUSTRATIVE EXAMPLES AND RESULTS

In order to evaluate the accuracy of the proposed Improved **AEM** and to illustrate the applicability of the method, a few examples are presented.

Example 1: Long Span beam steel beam under static load condition

The first example is the 2-D steel beam of 12.00 m span. The Dimensions, supports, loading conditions, and cross section are shown in **Fig. 5**. The defection at the mid span of the beam was calculated by using both previous **AEM** and improved **AEM** versions. The Young's Modulus is assumed as 200 GPa and elastic analysis was performed using both of two models. Element size is taken as total height of the cross section in **IAEM** case. The ratio between outer and inner springs' stiffness was taken as 20 (the same ratio between flange width and web thickness). However, since the thickness of each element in **AEM** is constant the element size it is taken as flange thickness in previous version of **AEM**. The results are compared to the theoretical results of the elastic structure. The theoretical relation between the maximum displacement (Δ) and applied load (P) at the mid span can be obtained simply from **Eq. 8.**

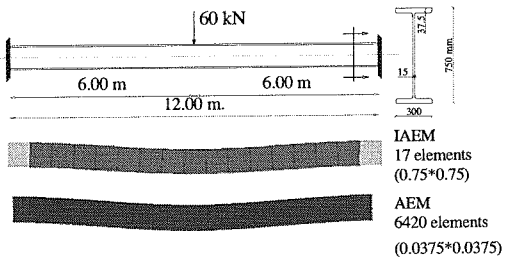

Fig. 5 Fixed Beam Loaded in Mid-span

$$\Delta = \frac{PL^3}{192EI} + \frac{PL}{4GA_s} \tag{8}$$

where L is the span length; I is the moment of inertia; and As is shear area which equal the area of web in I beam cross section in this case. A brief comparison between **AEM** and **IAEM** is listed in **Table 1**. The percentage of error in the maximum displacement is also shown in the table. From that table we can see that even by using less number of elements, the accuracy was much better with the **IAEM** compared with **AEM**.

Table 1 Comparison between AEM and IAEM Model results

	Required No. of elements	Element size (Cm^2)	No. of D.O.F	CPU Time Required	Deflection (mm)	% Error Comparing with theoretical value
AEM	6420	3.75*3.75	19140	154 sec	1.138	9.30%
IAEM	17	75*75	45	Less than one sec.	0.987	5.20 %

Example 2 Ten-story One-bay Frame

Another example to evaluate the accuracy of the proposed method, a two-dimensional ten-story-one pay frame structure was examined. The frame dimensions, supports, loading conditions, and cross section are shown in **Fig. 6**. By using our improved method, only 352 elements are used to simulate the structure. However if we use the previous version of AEM this number will rise to 43,170 elements. This means that the new method reduces the number of elements to be less than 1.00 % from those must be used with a previous version. **Table 2** presents results for the static lateral load analysis under linear load condition. The comparison with Finite element program (**SAP2000**)[17] is excellent.

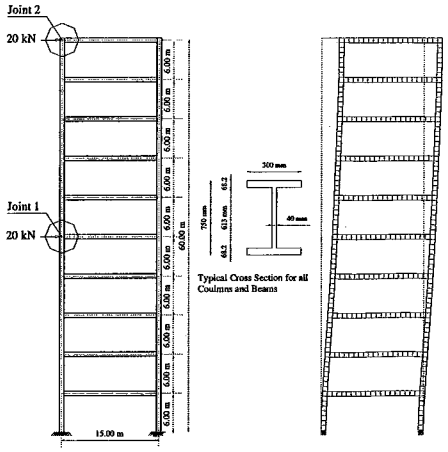

Fig. 6 Geometry and loading

Table 2 Comparison Results for Static Lateral Loads

	FEM	Improved AEM			Difference (%)
Horizontal Displacement At 5th floor level (mm) (Joint 1)	8.92	K_{out} / K_{in}	7.5	8.74	2.04
			6.8	8.94	0.22
Horizontal Displacement At 10th floor level (mm) (Joint 2)	14.95		7.5	14.66	1.93
			6.8	14.98	0.20

Another feature can be used with the IAEM, the error can also be reduced by changing the ratio between outer and inner springs' stiffness. According to **Table 2**, the error can be reduced to almost zero by changing the ratio between outer to inner stiffness from 7.5 to new value of 6.8. That feature can be used to optimize the difference between **IAEM** and **FEM** in the linear static case to start dynamic or nonlinear analyses with model to get a reasonable error ratio according to the required analyses.

Example 3: Dynamic analysis of Fifteen-story Two-bay Frame

In order to evaluate the accuracy of **IAEM** in dynamic analysis, a 15 story- two bay two-dimensional frame structure (presented in **Fig. 7**) is considered in this study. All the beams and column are assumed

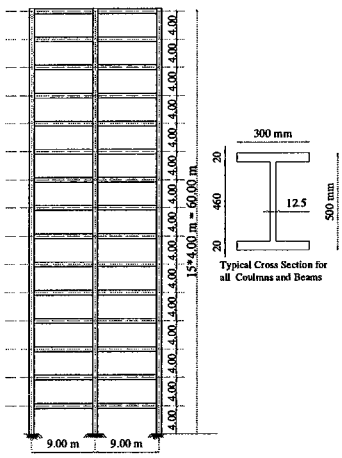

Fig. 7 Geometric and Cross Section

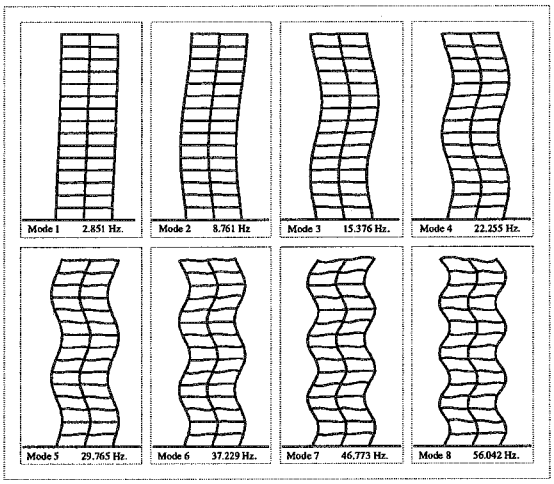

Fig. 8 First Eight modes calculated using Improved AEM

to have the same I-beam section represented in **Fig. 7**. Young's modulus of 200 GPa is used. The analysis is performed using 870 elements; however 543,750 elements should be used to simulate the same structure by using previous version of **AEM**. The model analysis is performed directly on the linear constant stiffness. The fundamental frequencies of the structure are calculated and listed in **Table 3**. The first 8 modes, obtained from IAEM and **SAP 20001**[7], are close and maximum 1.63 % difference has been observed. Those eight mode shapes are shown in **Fig. 8**.

Table 3: The Results of Model Analysis (Frequency, Hz)

Mode	1	2	3	4	5	6	7	8
FEM	2.817	8.627	15.129	21.903	29.316	37.229	46.253	55.320
IAEM	2.851	8.761	15.376	22.255	29.765	37.229	46.773	56.042
Difference %	1.21 %	1.55 %	1.63 %	1.61 %	1.53 %	0.00 %	1.12 %	1.31 %

The verification examples indicate that **IAEM** shows a good agreement with both theoretical and finite element results in linear static and dynamic load condition. Moreover, less computational effort and a wider applicability for structural analysis have been noted than conventional discrete element methods.

PROGRESSIVE FAILURE ANALYSIS OF STEEL HIGH-RISE BUILDING

Structural configuration and modeling

A 30 story steel frame building is analyzed in this part. The structural configuration of the building is shown in **Fig. 9**. The typical story height is 4.00 m. **Table 4** presents the section properties of the steel frame. The frame was designed to resist lateral load due to wind and seismic ground motions. The loading of 100% dead load plus 25 % live load is related to a requirement by GSA (2000)[18] for evaluating a building performance under severe fire conditions. The **IAEM** model was employed in this analysis. The main purpose of the analysis is to check the reliability of the proposed method and to check if the progressive failure will occur due to partial damage beyond one story level.

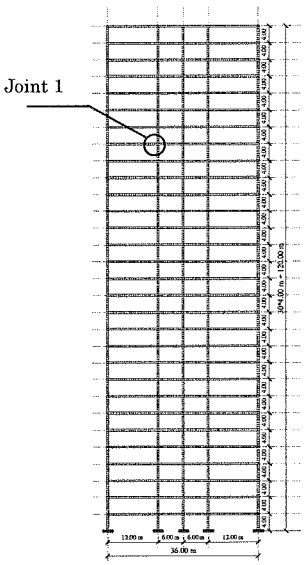

Fig. 9 Frame under study

Table 4 Section Properties

	A_n (m^2)	A_s (m^2)	I (m^4)
Beam members	0.0336	0.0115	1.514E-3
Columns form 1st to 10th level	0.4630	0.0159	2.003E-3
Columns form 11st to 20th level	0.0331	0.0117	1.480E-3
Columns form 21st to 30th level	0.0250	8.80E-3	1.117E-3

Progressive collapse analysis

According to the analysis, the results of using **IAEM** are shown in **Fig. 10**. The history of failure of the steel frame structure is presented. The collapse has been assumed to be due to fire at 22nd floor level. From the figure, we can see that the local failure, at that floor level, produced complete failure to the whole structure. The stages of this collapse can be summarized as follows:

- The collapse initiated due to high reduction in steel stiffness and strength of a part of 22nd floor level and a part of attached columns at that level. That reduction is similar to that which occurs due to the softness of steel metal when it is exposed to fire.
- The weakness and deformation cause the joist to separate form column at **Joint 1** presented in **Fig. 9**. Due to reduction in the stiffness at that location, the attached beams had extra deformation and finally that joint is totally damaged.
- The damage to the joist produced failure to the attached structural steel elements and also changed the buckling condition of some columns. That damage also caused redistribution of loading on many the structural elements.

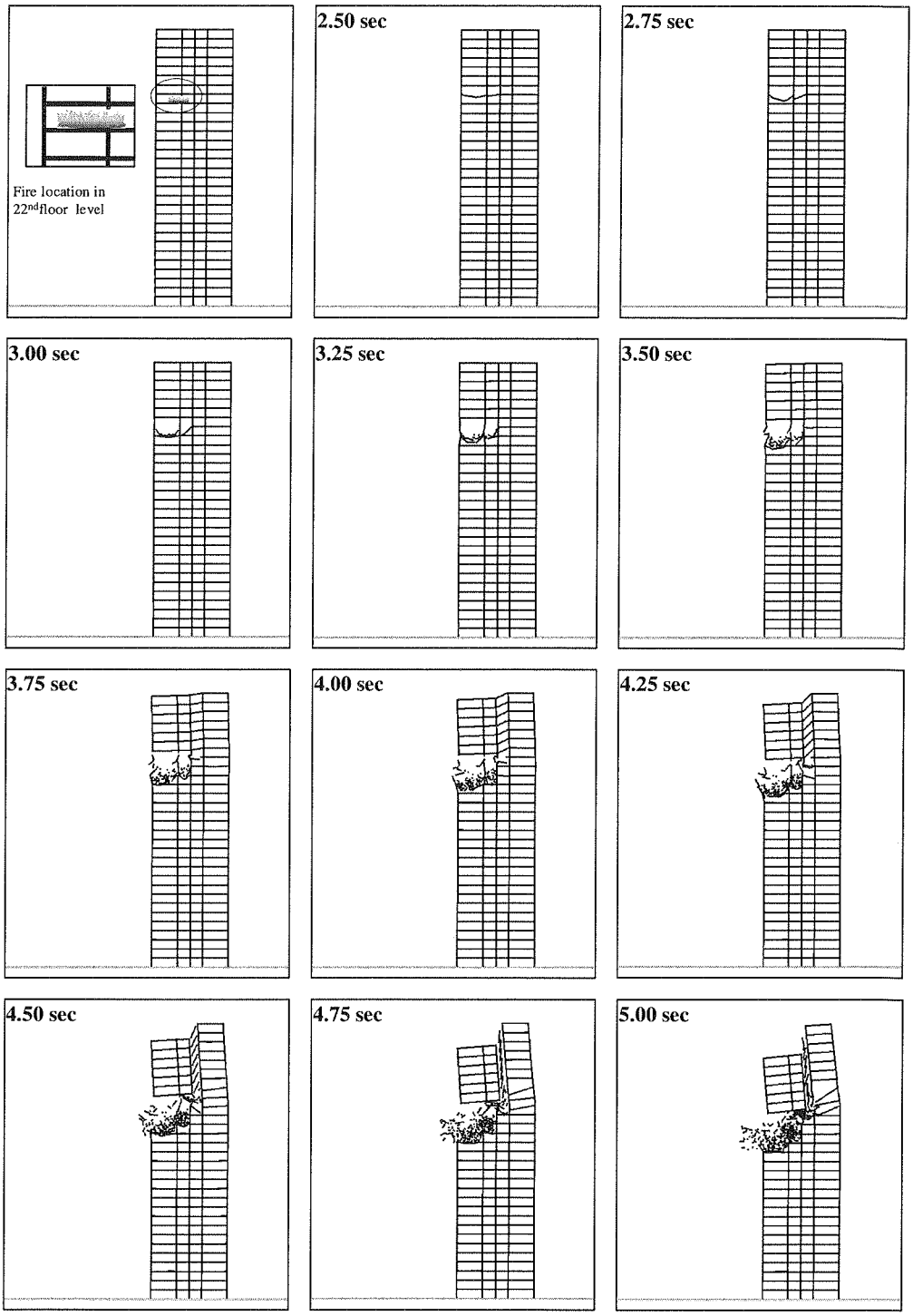

Fig. 10 (a) Failure Process for the Model High-rise Steel Structure Due to Sevier Fire

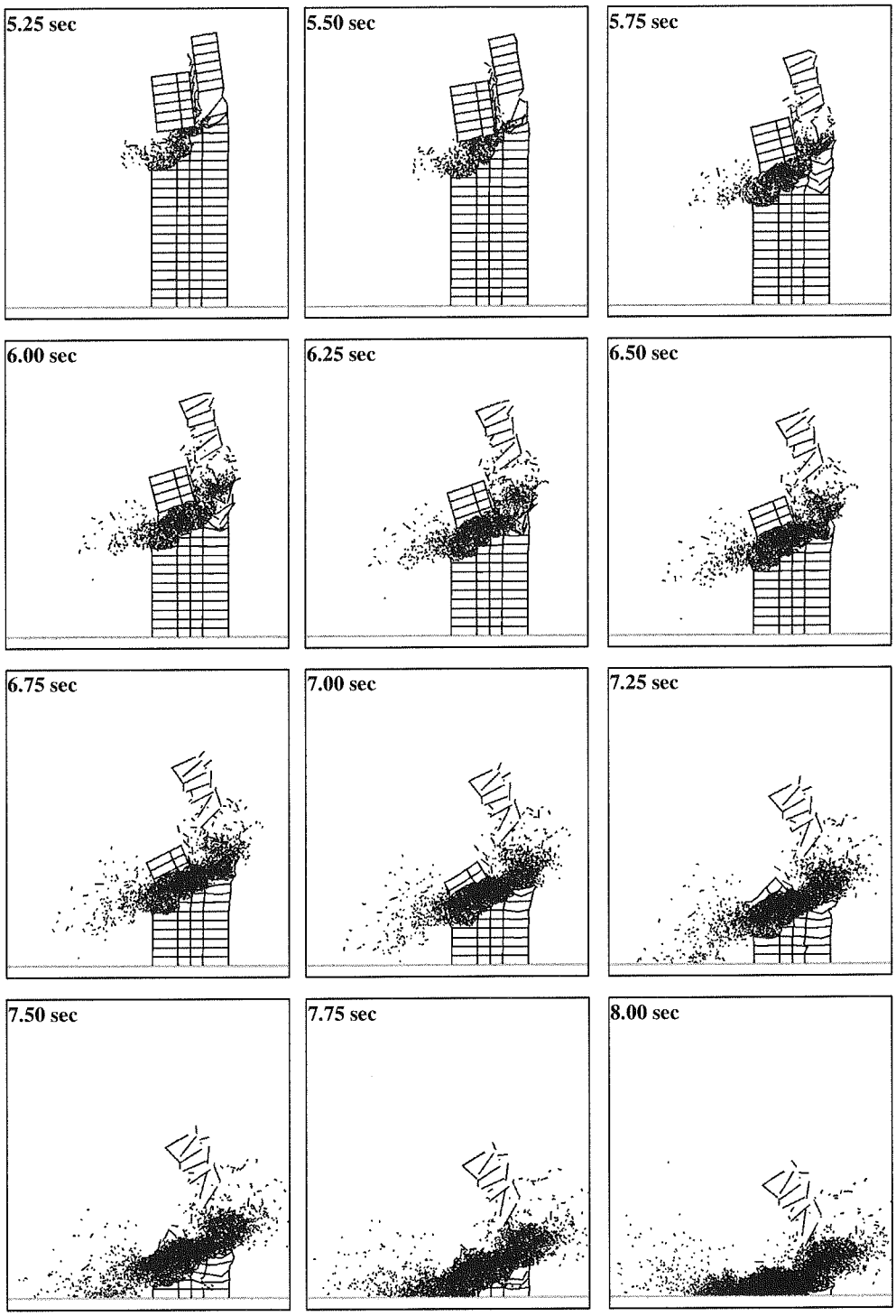

Fig. 10 (b) Failure Process for the Model High-rise Steel Structure Due to Sevier Fire

- When the columns or floor connections failed, the structural loading was no longer static, but dynamic. Once one floor fell onto another, it was a domino effect. The impact of one floor falling on the floor below creates a huge amount of force. As each floor fell, this force would increase until the bottom. Even if all the building structure below had been intact, the sudden impact of such a weight could not be sustained by the lower portion of the building that had been designed for static (steady, weight bearing) loads.
- The numerical simulation shows the mechanism of failure of a high rise steel structure under the effect of severe fire condition. The analysis explains how partial damage in certain structural element can produce total collapse of the building. The numerical simulation is qualitatively similar to the recorded sequence of collapse of North Tower in World Trade Centre, shown in **Fig. 11**.

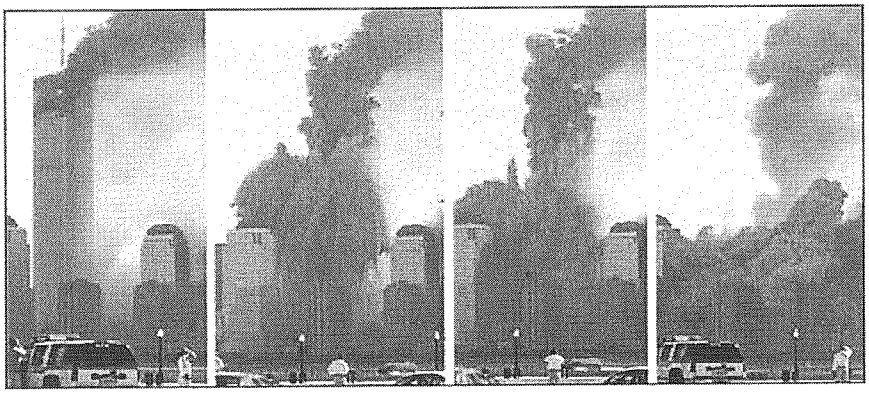

Fig. 11 Sequence of collapse of North Tower (Photo from CNN)

CONCLUSIONS

This paper presents Improved Applied Element Method (IAEM), a new proposed method for analyzing high rise building structures. The improved method requires less computer time and effort to model a structure. The verification examples indicate that IAEM has better accuracy, need less computational effort, and has a wider applicability for structural analysis, especially for studying high rise steel buildings than conventional methods.

IAEM is introduced to follow the collision behavior of the structural elements during failure. It is very difficult, or practically impossible, to follow such behavior using the methods in which the material is continuous, like FEM and BEM. The case study that represented in this paper provides to some extent the mechanism of progressive collapse of high-rise buildings. The failure mechanism for that example is similar to the collapse mechanism of the North Tower in World Trade Centre tower.

Simple two-dimensional analysis tools such as that adopted in this paper can be used to judge in a qualitative and quantitative the damage tolerance of buildings. It can also use to achieve better understanding the response of structure to ground motions, impact, fire, and blasting hazards.

REFERENCES

1) Crawford, J., Houghton, D., Dunn, B., and Karns, J. (2001). "Design Studies Related to the Vulnerability of Office Buildings to Progressive Collapse due to Terrorist Attack", Research Report TR-01-10.1, Karagozian & Case Structural Engineers, Glendale, California.
2) Zdenek P. Bazant and Yong Zhou. (2001). "Why Did the World Trade Center Collapse? —Simple Analysis," J. Engineering Mechanics ASCE, (September 28, 2001), also www.tam.uiuc.edu/news/200109wtc/

3) General Services Administration. (2000). "Progressive floor collapse analysis and design Guidelines for new federal office building and Modernization projects"
4) Steven Ashley, (2001). "When the Twin Towers Fell," Scientific American Online (October 9, 2001); www.sciam.com/explorations/2001/100901wtc
5) Meguro, K., Iwashita, K., and Hakuno, M. (1991). "Fracture analyses of structures by the modified distinct element method." Structural Eng./Earthquake Eng., JSCE, 6(2), 283s–294s.
6) Meguro, k. and Tagel-Din, H. (2001). "Applied Element Simulation of RC Structures under Cyclic Loading." ASCE, Vol. 127, Issue 11, pp. 1295-1305.
7) Meguro, k. and Tagel-Din, H. (2000). "Applied Element Method for Structural Analysis: Theory and Application for Linear Materials." Structural Eng./Earthquake Eng., JSCE, Vol. 17, No. 1, pp. 21-35.
8) Tagel-Din, H. and Meguro, K. (2000): "Applied Element Method for Simulation of Nonlinear Materials: Theory and Application for RC Structures, Structural Eng./Earthquake Eng., JSCE, Vol. 17, No. 2, 137s-148s.
9) Meguro, k. and Tagel-Din, H. (1999). "Simulation of Buckling and Post-Buckling Behaviour of Structures Using Applied Element Method." Bulletin of Earthquake Resistant Structure Research Center, Institute of Industrial Science, No. 32.
10) Tagel-Din, H. and Meguro, K. (2000). "Applied Element Method for Dynamic Large Deformation Analysis of Structures." Structural Eng./Earthquake Eng., JSCE, Vol. 17, No. 2, pp. 215s-224s.
11) Tagel-Din, H. and Meguro, K. (2000). "Analysis of a Small Scale RC Building Subjected to Shaking Table Tests using Applied Element Method." Proceedings of the 12th World Conference on Earthquake Engineering, New Zealand.
12) Tagel-Din, H. and Meguro, K. (1999). "Applied Element Simulation for Collapse Analysis of Structures." Bulletin of Earthquake Resistant Structure Research Center, Institute of Industrial Science, The University of Tokyo, No. 32.
13) Ramancharla, P. and Meguro, K. (2001). "Numerical modelling of dip-slip faults for studying ground surface deformation." Bulletin Earthquake Resistant Structure Research Center, No.34, pp.107-112.
14) Pandey B. and Meguro K. (2002). "Applied element simulation of masonry wall behaviour under in-plane lateral loading." Proceedings of the 4th International Summer Symposium, JSCE, pp.107-110.
15) Chopra K. (1995). "Dynamic of structures. Theory and applications to the earthquake engineers".
16) Meguro K. and Tagel-Din H. (2002). "Applied Element Method used for large displacement structural analysis." Journal of Nature Diaster Science, Vol. 24, No. 1, 25-34.
17) CSI (2000), "SAP2000- intergraded Finite Element Analysis and Design of Structures." Version 7.4, Computer and Structures, Inc., Berkeley, CA
18) General Services Administration (2000). "Progressive floor collapse analysis and design guidelines for new federal office building and modernization projects"